International Journal of Advanced Engineering Research and Science (IJAERS)
Peer-Reviewed Journal
ISSN: 2349-6495(P) | 2456-1908(O)
Vol-8, Issue-6; Jun, 2021
Journal Home Page Available: https://ijaers.com/
Article DOI: https://dx.doi.org/10.22161/ijaers.86.34

Solution of AePW-2 Test Cases Using Open-Source Code

Henrique Matos Campos, Filipe Augusto Sintra Lazzarini, Aluisio Viais Pantaleão

Department of Mechanical Engineering, School of Engineering, São Paulo State University (Unesp), Brazil

Received: 03 May 2021;

Received in revised form: 04 Jun 2021;

Accepted: 18 Jun 2021;

Available online: 24 Jun 2021

***Keywords*— CFD, SU2, AePW-2, Open-source code, BSCW.**

***Abstract*—** *The analyses presented in this paper are focus on the solution of cases 1 and 3A proposed by the second Aeroelastic Prediction Workshop (AePW-2), using an open-source CFD code. The reference cases presented by AePW-2 analyze the transonic flow around a Benchmark Supercritical Wing (BSCW). AePW-2 Test case 1 consists of a forced oscillation problem with Mach number of 0.7 and angle of attack of 3 deg, while AePW-2 Test case 3A analyzes a flow with Mach number of 0.85 and angle of attack of 5 deg, being that an unforced and unsteady problem. In the study, we simulated both test cases using the software SU2, being the results validated by comparison with experimental data provided by AePW-2. The results matched with accuracy with the experimental data and presented a good response for the analyses of AePW-2 test case 3A, proving the software capability of capture the physical phenomena involved in this type of flow.*

I. INTRODUCTION

Computational Fluid Dynamics (CFD) evolved a lot during the past two decades. To keep the improving state art of CFD, institutions around the world are developing workshops, among them, and Aeroelastic Prediction Workshop series (AePW) stands out, [1] provides more information about AePW.

The focus of the first edition of the AePW workshop series was the solution of unsteady aerodynamics problems over three different wing geometry (the Rectangular Supercritical Wing, the Benchmark Supercritical Wing (BSCW) and High Reynolds Number Aero-Structural Dynamics (HIRENASD)). In its second version, AePW focused on the analyses of problems involving flutter over the BSCW wing.

Since 2016, all the studies that presented a complete solution of AePW-2 test cases used proprietary codes or in-house codes, as seen in [2] and [3].

More recent studies, like [4], presented the solution of the test cases and expanded these, testing the influence of parameter variation but these also using in-house codes.

However, proprietary and in-house codes present some limitations for academia. In this context, open source becomes a better option. But nowadays, the full capabilities of open-source codes to solve complex flow problems are still unrecognized, with just a few papers given an overview of this topic.

Among the possibilities of open-source CFD codes, SU2 emerges as a relevant tool for aeroelastic studies since it is focused on aeronautics applications, as presented in [5].

In [6], the developers of SU2 presented more details of the software architecture and capabilities to solve the flow problem proposed by two different full-aircraft configuration test cases. The focus of [6] was to prove the capability of the software to solve industry-sized problems. But for the current study, the principal importance of [6] was proving that SU2 was capable of solving transonic flow problems over complex geometries since one of the test cases validated was the flow over DLR-F6 Transonic Aircraft.

According to [7], the developers of SU2 focused their efforts on verifying the capabilities of the software to solve different test cases of interest in computational

aeroelasticity. The study of [7] analyzed flows over NACA 0012 airfoil, Isogai wing section, BSCW wing, and also presenting the benchmark problems solution for fluid-structure interaction (FSI). The importance of the research of [7] for the current study was the analysis of the BSCW wing test cases, which indicates the capabilities of SU2 to solve the test cases of AePW-2.

In a more recent study of SU2 capabilities of solving transonic flows, [8] uses SU2 to develop a methodology capable of providing the flow response to small-amplitude periodic deformations in a structure. This methodology was developed using NACA 64A010 airfoil in transonic flow conditions and validated by testing it in an Isogai wing section and an AGARD 445.6 wing. The results evaluated by [8] were accurate when compared with experimental data and other numerical simulation results, reinforcing SU2 capabilities.

Verified the SU2 capability of solving transonic flows. The current study aims to expand the usage of open-source software to solve complex flow problems of interest for aeroelastic analysis. The objective proposed was achieved by analyzing the SU2's ability to solve test cases 1 and 3 presented in AePW-2 and by comparing the results obtained numerically with the experimental data provided by the workshop.

II. METHODOLOGY

AePW-2 uses the Benchmark Supercritical Wing (BSCW) for all the analysis proposed, Fig. 1:. presents the BSCW geometry view and its cross-section, a SC(2)-0414 airfoil. This rectangular wing has a chord of 0.4064 m, a span of 0.8128 m, a reference area of 0.3303 m², and a moment reference in (0.1219, 0, 0) m.

The BSCW configuration presents geometric simplicity, allowing to set the focus of AePW-2 on flow behavior.

[9] provided the experimental data of wind tunnel analysis for test cases 1 and 3A of AePW-2, being these evaluated for a cross-section of the wing, distancing 0.48768 m from the wing root. Table 1 synthesizes the information about the test cases verified in the current study, used to test SU2 capabilities.

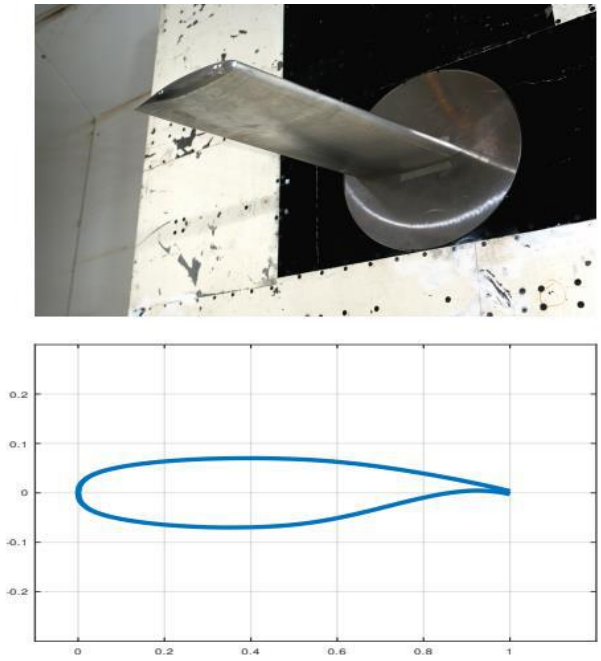

Fig. 1: Benchmark Supercritical Wing (BSCW) geometry used by AePW2 (presented in [1]).

Table. 1: Test Cases Proposed by AePW-2.

	Case 1	Case 3A
Mach Number (Ma)	0.7	0.85
Angle of Attack (AoA)	3°	5°
Fluid	R-134a	R-134a
Data type	Forced Oscillation	Unforced Unsteady
Reynolds Number (Re)	$4.560 \cdot 10^6$	$4.560 \cdot 10^6$
Freestream Velocity (V)	118.0588 m/s	118.0588 m/s
Speed of Sound (c)	168.6556 m/s	168.6556 m/s
Temperature (T)	304.2128 K	304.2128 K
Density (ρ)	1.1751 kg/m^3	1.1751 kg/m^3
Sutherland Constant (C)	243.3722 K	243.3722 K
Reference dynamic viscosity (μ_{ref})	$1.1165 \cdot 10^{-5}$ Ns/m^2	$1.1165 \cdot 10^{-5}$ Ns/m^2
Reference Temperature (T_{ref})	273 K	273 K

All the experimental data for the test cases presented in Table 1 are from NASA Langley Transonic Dynamics

Tunnel (TDT). The test case 3 points to shock-induced separated flow in the upper surface and the aft portion of the lower surface for Ma = 0.85 and AoA = 5°.

2. 1. MATHEMATICAL MODEL

Since all the analyzed test cases use R-134a is possible to consider the fluid as an ideal gas. Adopting this hypothesis is possible to create a correlation between the dynamic viscosity (μ) and the absolute temperature (T), via Sutherland's law, defined in (1).

$$\mu = \mu_{ref}\left(\frac{T}{T_{ref}}\right)^{3/2}\frac{T_{ref}+S}{T+S} \tag{1}$$

In all the AePW-2 test cases, the fluid flow is considered turbulent. To model the turbulence, we adopted the Reynolds-averaged Navier–Stokes equations (RANS). With that approach, the governing equations fall on a closure problem. To solve this, we used a turbulence model.

Based on the study of [3], was used the Spalart-Allmaras Turbulence Model for the analyses of case 1 in steady condition and case 3A. The Spalart-Allmaras model is a one equation model defined according to [10] by the equation (2).

$$\frac{\partial\tilde{\nu}}{\partial t}+u_j\frac{\partial\tilde{\nu}}{\partial x_j}= c_{b1}(1-f_{t2})\tilde{S}\tilde{\nu}-\left(c_{\omega1}f_\omega-\frac{c_{b1}}{\kappa^2}f_{t2}\right)\left(\frac{\tilde{\nu}}{d}\right)^2 + \frac{1}{\sigma}\left[\frac{\partial}{\partial x_j}\left((\nu+\tilde{\nu})\frac{\partial\tilde{\nu}}{\partial x_j}\right)+c_{b2}\frac{\partial\tilde{\nu}}{\partial x_i}\frac{\partial\tilde{\nu}}{\partial x_i}\right] \tag{2}$$

Being the turbulence viscosity (μ_t) defined as:

$$\mu_t = \rho\nu f_{v1} \tag{3}$$

Where f_{v1} and χ are determined as:

$$f_{v1}=\frac{\chi^3}{\chi^3+c_{v1}^3} \tag{4}$$

$$\chi=\frac{\tilde{\nu}}{\nu} \tag{5}$$

For this turbulence model, the adopted boundary conditions are:

$$\tilde{\nu}_{wall}=0 \tag{6}$$

$$0.210438\cdot\nu_\infty \le \tilde{\nu}_{farfield} \le 1.294234\cdot\nu_\infty \tag{7}$$

Since the Spalart-Allmaras turbulence model is a one equation model, it is considerably faster than other models with more equations.

[10] presents the constants and auxiliary relations for the Spalart-Allmaras Turbulence Model.

For case 1 transient simulation, we considered the turbulence model proposed by [11], the shear stress transport, or k − ω SST, which is a two equations eddy-viscosity model. This formulation consists of a set of equations for turbulence kinetic energy and the specific dissipation rate equations complemented by the kinematic eddy viscosity equation, given by (8), (9), and (10).

$$\mu_T=\frac{\rho a_1 k}{max(a_1\omega;SF_2)} \tag{8}$$

$$\frac{\partial(\rho k)}{\partial t}+U_j\frac{\partial(\rho k)}{\partial x_j}=P_k-\beta^*k\omega+\frac{\partial}{\partial x_j}\left[(\mu+\sigma_k\mu_T)\frac{\partial k}{\partial x_j}\right] \tag{9}$$

$$\frac{\partial(\rho\omega)}{\partial t}+U_j\frac{\partial(\rho\omega)}{\partial x_j}=\frac{\gamma}{\nu_T}P-\beta\rho\omega^2+\frac{\partial}{\partial x_j}\left[(\mu+\sigma_\omega\mu_T)\frac{\partial\omega}{\partial x_j}\right]+2(1-F_1)\sigma_{\omega2}\frac{\rho}{\omega}\frac{\partial k}{\partial x_i}\frac{\partial\omega}{\partial x_i} \tag{10}$$

[11] presents more detail about the coefficients and auxiliary relations for the k − ω SST turbulence model.

2. 2. COMPUTATIONAL ANALYSIS

2. 2. 1. Mesh

We generated the mesh using the Ansys Mesh, from Ansys academic license, software details can be found in [12], and verify the uncertainty due to discretization calculating the Grid Convergence Index (GCI), following the procedure proposed by [13].

For all the meshes developed, we centered the wing profile in a semispherical farfield, as can be seen in Fig. 2. The figure also presents the boundary conditions adopted in the analysis. Table 2 shows the parameters used in the mesh generation for cases 1 and 3.

For case 1 grid convergence analysis, we developed the coarse, intermediary, and fine meshes present respectively: 156819 elements, 426703 elements, and 1184414 elements.

The obtained refinement factor was: 1.405 between the fine and the intermediary mesh; and 1.396 between the intermediary and the coarse mesh.

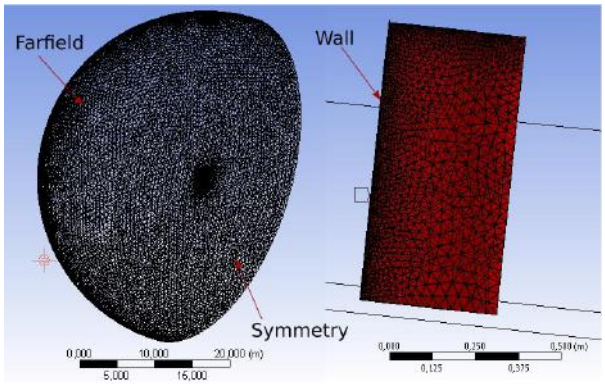

Fig. 2: Mesh developed for test case 1.

Table. 2: Test Cases Proposed by AePW-2.

Parameter	Case 1	Case 3A
y+	1	1
Aspect Ratio	1,2	1,2
Number of elements in the boundary layer	35	35
Farfield radius (m)	20	20
First element height (m)	$2{,}43 \cdot 10^{-6}$	$2{,}47 \cdot 10^{-6}$

Following the calculation procedure proposed by [13] we estimate uncertainty due to discretization using the GCI and obtained the results presented in Table 3.

Table. 3: Parameters obtained for estimate uncertainty due to the discretization of the BSCW wing.

Refinement factor r_{21}	1,405
Refinement factor r_{32}	1,396
Approximate relative error e_{a21}	0,93 %
Approximate relative error e_{a32}	13,12 %
Extrapolated relative error e_{ex21}	0,07 %
Extrapolated relative error e_{ex32}	1,03%
Convergence index GCI_{21}	0,085 %
Convergence index GCI_{32}	1,272 %

Comparing the parameters presented in Table 3 with the exhibit in [13], we saw that the convergence index allows the use of the intermediary mesh for all the calculations. Based on that result, we developed the meshes for case 3A the difference, in this case, was the use of a refinement box around the wing, as presented in Fig. 3.

With the adoption of a refinement box, we did a local refinement in the mesh to capture flow features of pressure distribution around the wing. The most dominant feature found in the flow is the shock-waves dynamics that should occur at the Mach number of 0,85. With this refinement, the mesh developed for case 3A had 1768317 elements, and the focus of this the upper region of the wing to capture the shock-wave dynamics.

2. 2. 2. Software

We used Ansys Mesh from Ansys License of Ansys 2017 for the mesh generation, [12] presents details about this software.

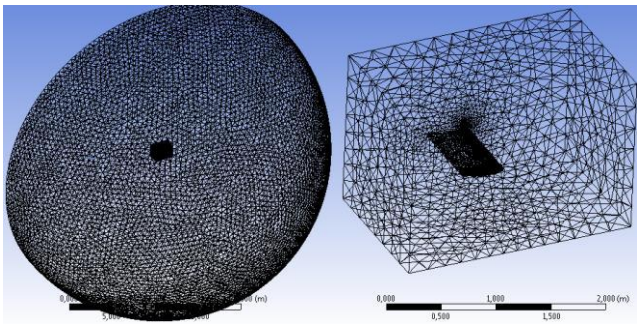

Fig. 3: Mesh developed for test case 3A.

For the numerical simulation, we used SU2 version v6.2.0 Falcon to solve the Navier-Stokes equations. [5] presents more detail about the software.

We evaluated the solution with the following settings: Green-Gauss numerical method to compute the gradient; FGMRES with ILU preconditioner to solve the linear system; JST as flow convective numerical method and Scalar Upwind as the turbulent convective numerical method.

For the post-process, we used Paraview 5.7.0. [14] provides details about Paraview.

III. RESULTS AND DISCUSSION

3. 1. Case 1

In Fig. 4. are presented the results obtained with the numerical simulation of test case 1 for the steady flow condition. For this test condition, we sampled 76 points over the analyzed section and compared them with the 35 points found in the experimental data provided by [1].

As can be seen in Fig. 4., the numerical data almost fit with the experimental data provided by AePW-2 for the lower surface of the airfoil.

For the upper surface, numerical and experimental data present the same behavior in the Cp curve but diverges in magnitude. This divergence in the upper surface occurs

because the tetra/prism mesh generated kept some lower quality elements in the region.

Also, Fig. 4. shows that on the trailing edge of the wing, the numerical simulation diverges from the experimental data. This problem occurs because of the sharper edge used in the geometry model. Due to that fact, the software couldn't generate good quality elements, leading to an increase in numerical error.

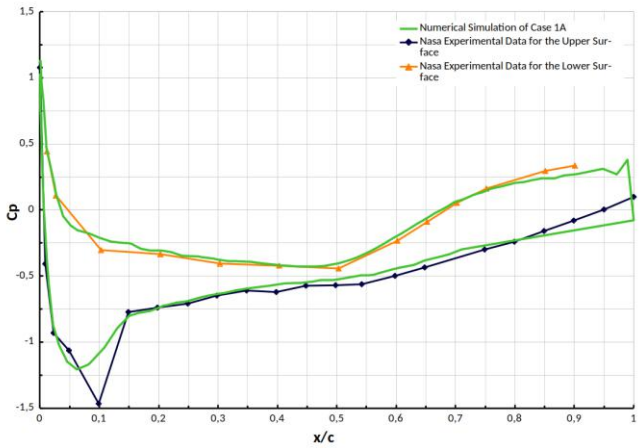

Fig. 4: Cp plot for numerical and experimental data of test case 1.

With the results, we concluded that SU2 could solve the steady transonic fluid flows with great accuracy since, in Fig. 4., we saw that most of the issues took place due to poor quality elements generate in some regions of the geometry.

The major problem found for the analysis was the mesh generation. This issue occurs due to SU2 uses meshes in SU2, CGNS, and NETCDF_ASCII formats, and just a few software develop great quality mesh in these formats.

During the study, we found that Ansys mesh was the only software capable of generating meshes for SU2. We also tested Gmsh, but at that time, it didn't generate proper meshes. For this reason, we used Ansys mesh to develop all the meshes for the studied test cases.

For case 1 transient condition, was verified the forced oscillation occurring over the BSCW wing. We simulated this condition with an oscillation frequency of 10 Hz and an angle of 1°. Fig. 5. presents the pressure coefficient evaluated with the numerical analysis, and we can compare this with the pressure coefficient found by [3] for the same test case, exposed in Fig. 6.

As can be seen in Fig. 5. and Fig 6. the results evaluated by the authors keep the same behavior as the results evaluated by [3].

The magnitude of the peak curvature is analogous to the one found in [3]. However, the curvature found by [3] presents two peaks, while the curves obtained by the authors present a single peak. Again the pressure coefficient next to the trailing edge was poorly represented in comparison with the found by [3].

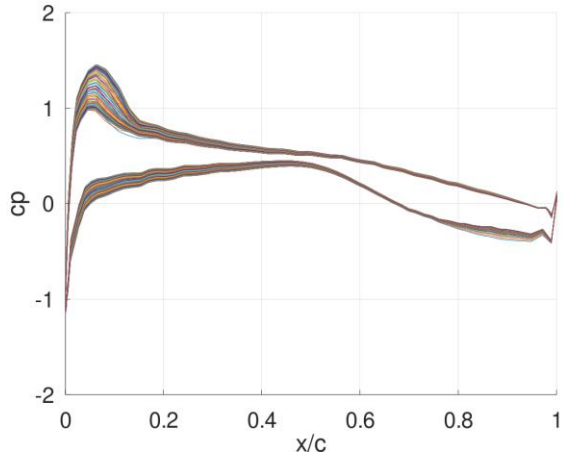

Fig. 5: Cp coefficients obtained by the authors for test case 1 transient condition.

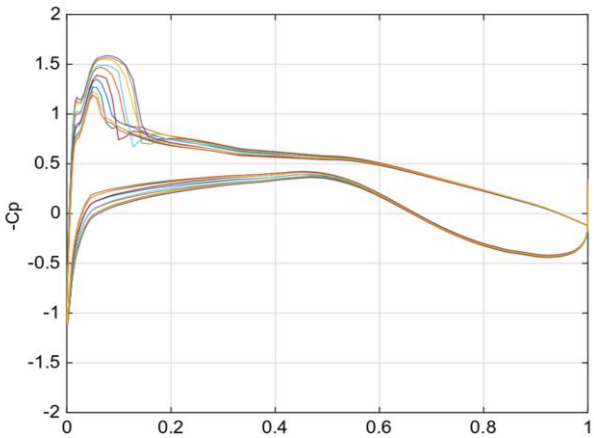

Fig. 6: Cp coefficients obtained by [3] for test case 1 transient condition.

Another way to see the behavior of SU2 is to plot the results in the frequency spectrum. AePW-2 presents the frequency response at 10 Hz for the sensors applied in the experimental tests. We can see a comparison between this response and the computational responses obtained by SU2 in Fig. 7. and Fig 8.

In Fig. 7. and Fig 8., we can see that the values obtained by SU2 are similar to the experimental evaluated by AePW-2, keeping the same shape and same peaks at upper and lower surfaces.

3. 2. Case 3A

Since case 3A consists of an unsteady problem, it was necessary to adopt a time step for developing the

interactions over time. For the analysis, we used a time step of $\Delta t = 10^{-4}$ s. Fig. 9. presents the results obtained for the SA model and Fig. 10. for the k−ω SST model.

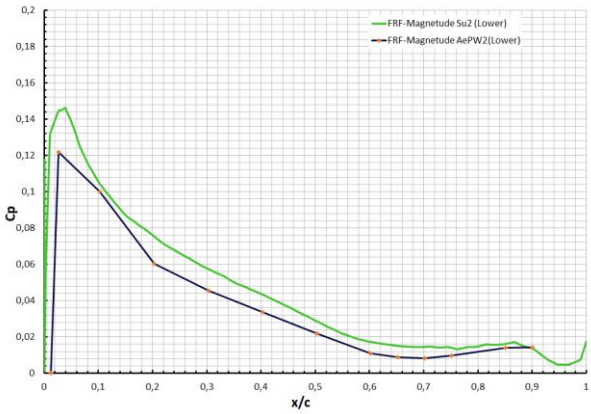

Fig. 7: Comparison between the magnitude frequency response at 10 Hz for the lower surface.

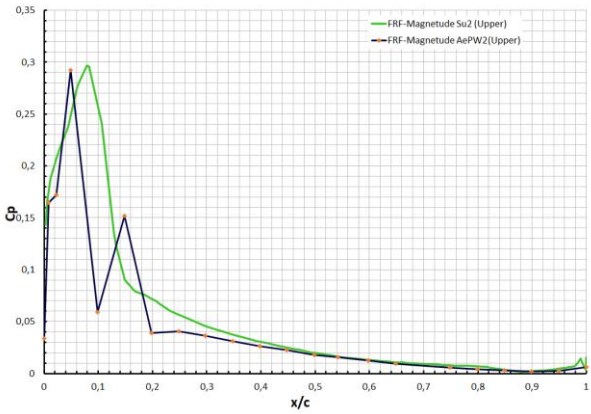

Fig. 8: Comparison between the magnitude frequency response at 10 Hz for the upper surface.

As presented in Fig. 9. and Fig. 10., the numerical results almost fit with the experimental data for this case. The difference found stays on the transition of the Cp that occurs next to x/c = 0.16, where the experiments present an abrupt fall of the Cp, while the numerical results exhibit a smooth transition.

Comparing case 3A and case 1 results, it is possible to see that the first presented more accuracy due to the mesh used.

Since case 1 consists of a flow with a low Reynolds number, and the problem occurs at a steady-state, the mesh for this case was coarser than case 3A mesh due to it doesn't use the refinement box. These simplifications into the mesh reduce the computational cost but sacrifice part of the solution's accuracy.

For case 3A, since the problem involves capture the shock wave dynamics over the wing was necessary to adopt local refinement techniques in the mesh generation. Due to the local refinement, we minimized the trailing edge problem found in case 1 and got a more accurate solution.

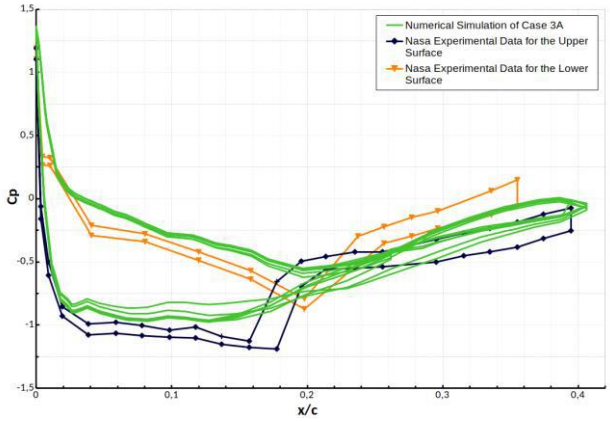

Fig 9: Comparison between Cp plot for numerical and experimental data of test case 3A using SA model.

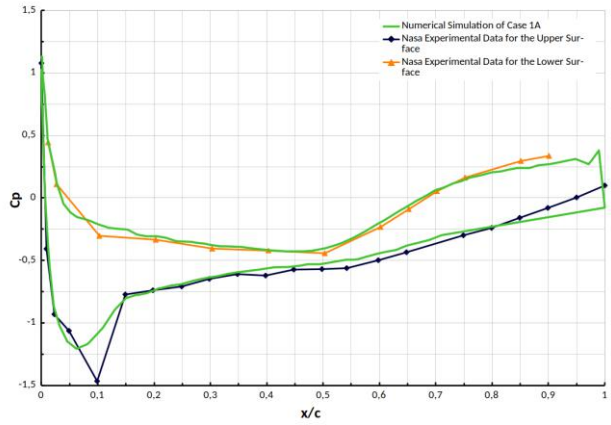

Fig 10: Comparison between Cp plot for numerical and experimental data of test case 3A using k−ω SST.

Another detail noticed is the difference evaluated by the turbulence models. While the SA model captured the Cp variation over time, as seen in Fig. 9., the k − ω SST wasn't capable of that, as presented in Fig. 10.

Also, Fig. 9. and Fig. 10. presents that despite both turbulence models represent the behavior of the flow over the wing adequately, but none captured the discontinuity presented by the shock wave.

IV. CONCLUSION

After all the analyses, we confirmed the capability of SU2 to solve transonic problems.

During the study, the principal limitation found was the generation of a proper mesh. Since SU2 native format is .su2, our first attempt was to use open-source mesh generators capable of generating meshes in this format.

None of the .su2 Open-source mesh generators tested generated meshes that provided good results for SU2.

Due to that, during the study were necessary to use another mesh format. In this case, was used the CGNS format, being the meshes generate by Ansys Mesh.

The results also present that the generated mesh impacts the accuracy of the simulation. Since a more refined mesh, like the one used for the numerical simulation of case 3A, was more accurate when compared with the coarse mesh generated for case 1, even considering that complexity of case 3A greater than case 1. This result also shows the importance of local refinement for unstructured meshes.

The analysis of case 3A presents that SU2 was capable of capture the shock wave dynamics. Also, the numerical results almost fit with the experimental data provided by the workshop AePW-2.

As observed in Fig. 9. and Fig. 10., the major problem found for the analysis was the capture of the abruptly falls off the Cp over the upper surface of the BSCW wing since the numerical simulation presents a smooth transition between the Cp curve while the experimental data shows a more abruptly fall.

ACKNOWLEDGEMENTS

This work has been possible in function of the São Paulo Research Foundation (FAPESP) grants, processes 2019/07947-0 (Regular Process).

This research was supported by resources supplied by the Center for Scientific Computing (NCC/GridUNESP) of the São Paulo State University (UNESP).

REFERENCES

[1] AePW-2. (2016). Aepw-2 homepage. Retrieved from https://nescacademy.nasa.gov/workshops/AePW2/public.

[2] Begnini, G.R., Spode, C., Pantaleão, A.V., Neto, B.G., Marcório, G.O., Pedras, M.H.J. and Bones, C.A., (2016). A comparison of cfd and aic-based methods for unsteady aerodynamics and flutter computations of the aepw-2 wing model. AIAA Aviation, vol. 34, No. 3123.

[3] Raveh, D.E., Yossef, Y.M. and Levy, Y., (2018). Analyses for the second aeroelastic prediction workshop using the eznss code. AIAA Journal, vol. 56, No. 1, pp. 387–402.

[4] Heeg, J. and Chwalowski, P., (2019). Predicting transonic flutter using nonlinear computational simulations. In International Forum on Aeroelasticity and Structural Dynamics. Savannah, Georgia.

[5] SU2 Foundation, (2020). Su2 official website. Retrieved from https://su2code.github.io/.

[6] Economon, T.D., Palacios, R., Copeland, S.R., Lukaczy, T.W. and Alonso, J.J., (2015). Su2: An open-source suite for multiphysics simulation and design. In AIAA Journal. AIAA, vol. 54. doi:10.2514/1.J053813.

[7] Sanchez, R., Kline, H.L., Thomas, D., Variyar, A., M., R., Economon, T.D., Alonso, J.J., Palacios, F., Dimitriadis, G. and Terrapon, V., (2016). Assessment of the fluid-structure interaction capabilities foraeronautical applications of the open-source solver su2. In VII European Congress on Computational Methods in Applied Sciences and Engineering.

[8] Güner, H., Thomas, D., Dimitriadis, G. and Terrapon, V., (2019). Unsteady aerodynamic modeling methodology based on dynamic mode interpolation for transonic flutter calculations. Journal of Fluids and Structures, vol. 84, pp. 218–232.

[9] AePW-2. (2016). Experimental data. Retrieved from https://nescacademy.nasa.gov/workshops/AePW2/public/BSCW/experimentalData.

[10] Rumsey, C., (2020). The spalart-allmaras turbulence model. Retrieved from https://turbmodels.larc.nasa.gov/spalart.html.

[11] Menter, F.R., (1993). Zonal two equation k-ω, turbulence models for aerodynamic flows. 24th Fluid Dynamics Conference.

[12] Ansys. (2020). Ansys fluent. Retrieved from https://www.ansys.com/products/fluids/ansys-fluent.

[13] Celik, I., Ghia, U., Roache, P., Freitas, C., Coleman, H. and Raad, P., (2008). Procedure for estimation and reporting of uncertainty due to discretization in cfd applications. Journal of Fluids Engineering, vol. 130.

[14] ParaView, (2015). Paraview official website. Retrieved from https://www.paraview.org/.